Published by
NIGERIAN SOCIETY OF PHYSICAL SCIENCES
Available online @ https://journal.nsps.org.ng/index.php/jnsps

J. Nig. Soc. Phys. Sci. 7 (2025) 2734

Journal of the Nigerian Society of Physical Sciences

Interaction of hydroxyapatite and chitosan with gentamicin and their antimicrobial activities: DFT and molecular docking approach

Nassima Bou-ydia*, Ben-issa El miraoui, Latifa Laallam, Ahmed Jouaiti

Laboratory of Molecular Chemistry, Materials, and Catalysis, Sustainable Development Team, Sultan Moulay Slimane University, Beni Mellal, Morocco

Abstract

Motivated by the potential use of hydroxyapatite and chitosan as drug delivery systems for the antibiotic gentamicin in the coating of metal implants, a theoretical study was conducted to investigate the interaction mechanisms among these three compounds, assess the stability of the resulting coating, and evaluate the inhibitory potential of chitosan and gentamicin against Protein A from Staphylococcus aureus. The results of this study demonstrate that hydroxyapatite, chitosan, and gentamicin exhibit a low HOMO-LUMO energy gap, indicating that electron transfer between their molecular orbitals can occur readily due to the molecules' structural flexibility. Additionally, chitosan shows a stronger binding affinity for gentamicin than hydroxyapatite, and both chitosan and gentamicin display a significant inhibitory effect against Protein A. Two theoretical approaches were employed: density functional theory using the B3LYP functional (Becke's three-parameter hybrid functional combined with the LYP correlation functional) and the 3-21G basis set, as well as a molecular docking study using the MOE software (version 2015). The docking simulations generated 30 binding poses, which were evaluated using the London dG scoring function and refined twice using the Triangle Matcher placement method.

DOI:10.46481/jnsps.2025.2734

Keywords: Hydroxyapatite, Chitosan, Gentamicin, Protein A

Article History :
Received: 07 March 2025
Received in revised form: 05 June 2025
Accepted for publication: 08 June 2025
Available online: 15 June 2025

© 2025 The Author(s). Published by the Nigerian Society of Physical Sciences under the terms of the Creative Commons Attribution 4.0 International license. Further distribution of this work must maintain attribution to the author(s) and the published article's title, journal citation, and DOI.

Communicated by: B. J. Falaye

1. Introduction

Corrosion and osteomyelitis are the most common complications associated with metal implants used in dental and surgical applications. Researchers have focused on these issues to develop effective prevention strategies and improve patient care [1, 2]. Osteomyelitis is a deep bone marrow infection characterized by interrupting blood flow around the infected area. It is often caused by surgical procedures or open fractures [3, 4]. The main bacterial agents responsible for osteomyelitis are Gram-positive species, particularly Staphylococcus aureus and Staphylococcus epidermidis [4]. In S. aureus, the cell wall protein A is the most extensively studied receptor [5], as it binds specifically to the Fc region of immunoglobulin G (IgG) in various mammalian species [6]. Numerous studies have focused on developing drug-delivery systems to combat bacterial infections associated with metallic implants [7]. Among the materials used, hydroxyapatite (HAP) stands out as one of the most widely adopted coating polymers due to its excellent biocompatibility and non-toxicity [7].

Furthermore, extensive research has demonstrated that combining HAP with chitosan (CHI) enhances the coating's

*Corresponding author Tel. No.: +21-268-934-2031.
Email address: nassima.bou-ydia@usms.ma (Nassima Bou-ydia)

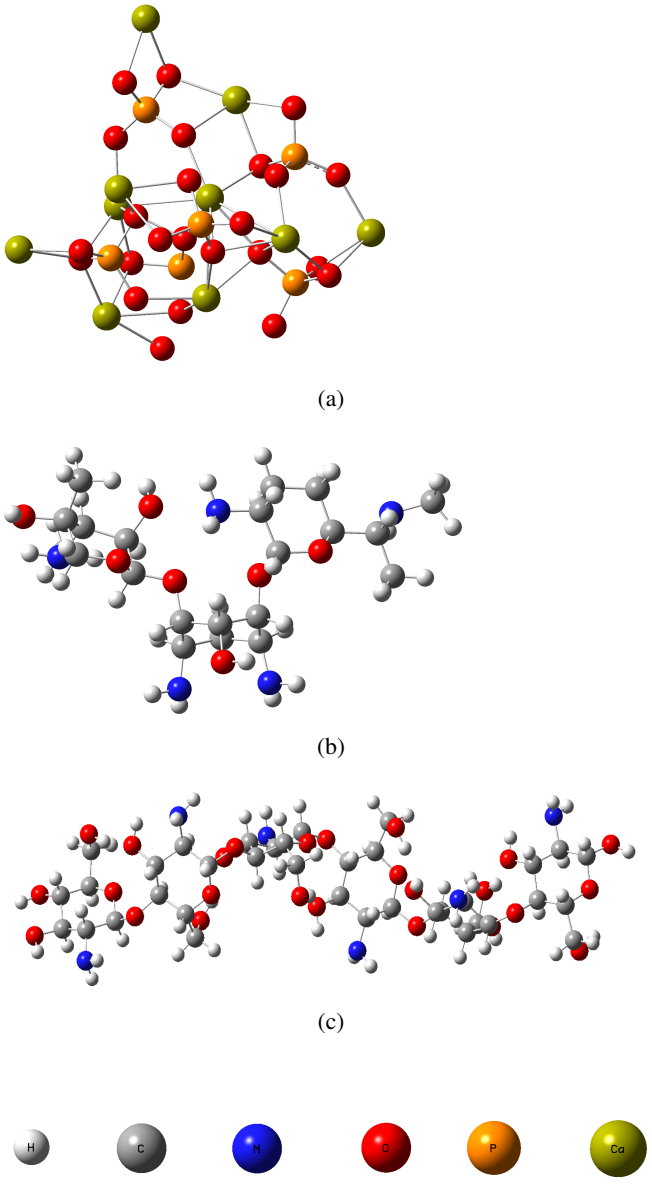

Figure 1: Optimized structures of (a) Hydroxyapatite, (b) Gentamicin, and (c) Chitosan.

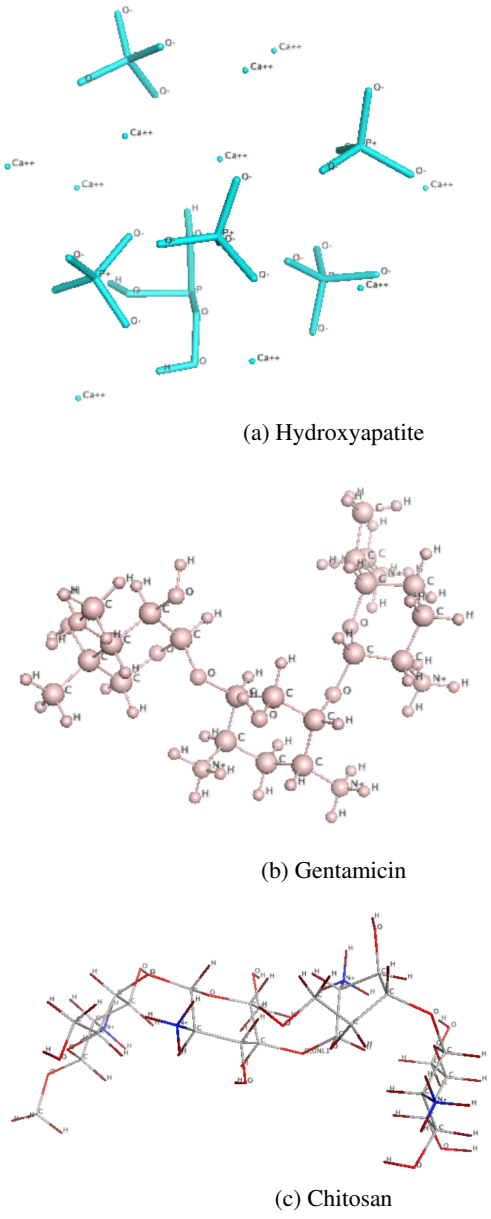

Figure 2: The 3D structures of HAP, CHI, and GEN obtained from the MOE docking (vs. 2015).

performance. Chitosan offers several advantages, including low allergenicity, notable antimicrobial activity, and excellent film-forming properties [7, 8]. Given that osteomyelitis is a bacterial infection primarily caused by S. aureus, incorporating an antibiotic into the coating is essential. Gentamicin (GEN) is commonly used to treat osteomyelitis [7, 8]. Therefore, this research aimed to evaluate the interactions between gentamicin, HAP, and chitosan, as well as to assess the inhibitory potential of CHI and GEN against Protein A. The theoretical approaches employed in this study included density functional theory (DFT) and molecular docking using the MOE software. DFT is one of the most commonly used methods in theoretical chemistry due to its high accuracy and efficiency when modeling large molecular systems [9–13]. DFT calculations were carried out on HAP, CHI, and GEN to optimize the geometry of the three compounds using the B3LYP functional with the 3-21G basis set [14]. Following geometry optimization, MOE docking simulations were performed to predict the stability of the coating through the analysis of interactions between the polymers and the antibiotic. The docking study also aimed to estimate the inhibitory effect of CHI and GEN on Protein A [15]. This work provides valuable theoretical insights to support and complement experimental findings, enrich the existing scientific literature, and offer guidance for future research and development in the field.

- HA with CHI interaction (Table 3)

Residue	%
ALA	13.00
ASN	13.00
LEU	11.66
GLN	10.00
LYS	10.00
GLU	8.30
ASP	6.66
PRO	5.00
SER	5.00
PHE	5.00
ILE	3.33
THR	1.66
HIS	1.66
ARG	1.66
GLY	1.66
TYR	1.66

Protein A

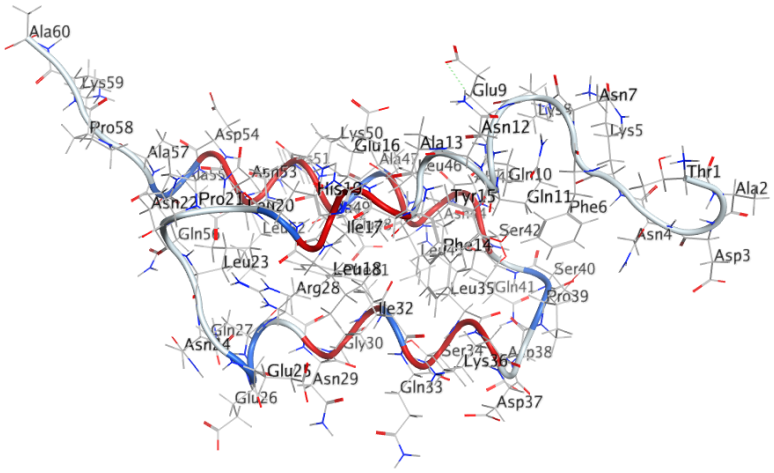

Figure 3: 3D modeled structure of protein A and % residue.

Table 1: The representation of the molecular orbitals of HAP, CHI, and GEN optimized and their HOMO-LUMO energy levels.

Hydroxyapatite	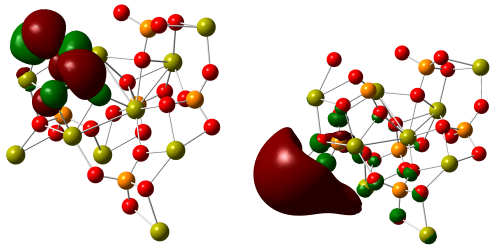	
	HOMO ⟶ LUMO	
	$E = -0.17835$ eV	$E = -0.02921$ eV
Chitosan	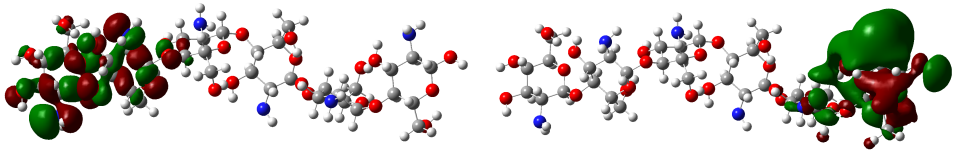	
	HOMO ⟶ LUMO	
	$E = -0.36480$ eV	$E = 0.22794$ eV
Gentamicin	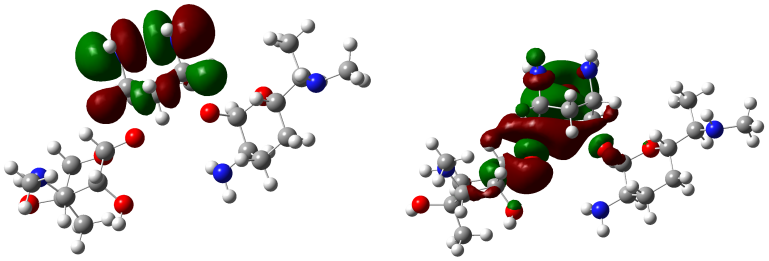	
	HOMO ⟶ LUMO	
	$E = -0.17835$ eV	$E = 0.05253$ eV

- HA with GEN interaction (Table 4)
- CHI with GEN interaction (Table 5)

Table 2: $\Delta E = E_{LUMO} - E_{HOMO}$, GAP energy and reactivity indices, hardness (η), and softness (S) for the studied compounds.

Compounds	ΔE [eV]	Gap	η	S
HAP	0.149	-0.149	0.0745	13.422
CHI	0.592	-0.592	0.296	3.378
GEN	0.247	-0.247	0.1235	8.097

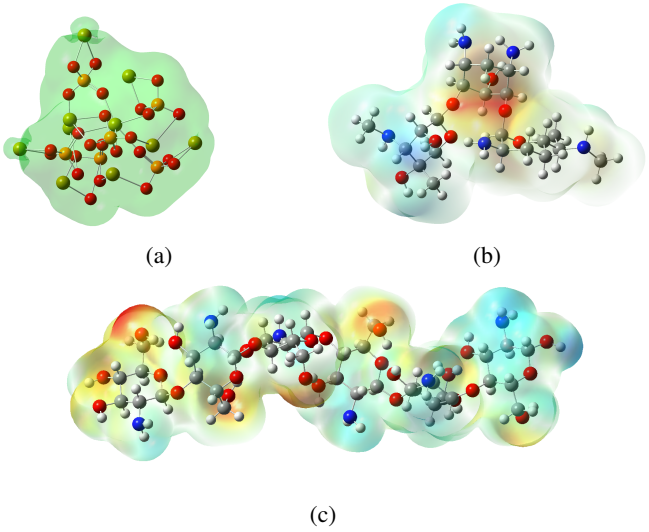

(a) (b) (c)

Figure 4: Electrostatic potential map (MEP) for HAP (a), GEN (b), and CHI (c).

2. Computational studies

2.1. Conformational strategy

All calculations were performed using Gaussian 09 software [16], and molecular structures were visualized using GaussView 5.09 [17]. The frequency calculations confirmed the absence of imaginary frequencies, indicating that all optimized structures correspond to true energy minima. Density Functional Theory (DFT) accounts for electron correlation by evaluating the interaction of an electron with the total electron density. DFT orbitals are constructed using basis functions, and among the available methods, B3LYP (Becke's three-parameter hybrid functional combined with the LYP correlation functional) is one of the most widely applied [9]. In this study, DFT calculations were performed on hydroxyapatite (HAP), chitosan (CHI), and gentamicin (GEN) using the B3LYP functional and the 3-21G basis set [14]. The optimized structures of all the studied compounds are presented in Figure 1. Furthermore, key electronic parameters such as the HOMO-LUMO energy gap (ΔE), absolute hardness (η), and softness (S) were calculated at the B3LYP/3-21G level [14, 18].

The difference between the HOMO and the LUMO is the gap energy [19]:

$$\text{Gap} = \text{HOMO} - \text{LUMO}. \quad (1)$$

The hardness η is:

$$\eta = (\text{LUMO} - \text{HOMO})/2, \quad (2)$$

the inverse of hardness is softness (S):

$$S = 1/\eta. \quad (3)$$

2.2. Molecular operating environmental docking (MOE) approach

A 3D ligand structure consisting of hydroxyapatite (Symbol: HAP, Formula: $Ca_5HO_{13}P_3$), chitosan (Symbol: CHI, Formula: $C_{56}H_{103}O_{39}$), and gentamicin (Symbol: GEN, Formula: $C_{21}H_{43}N_5O_7$) was used in this study to evaluate their inhibitory potential against Protein A of Staphylococcus aureus. The 3D structure of Protein A (PDB ID: 1BDC - Immunoglobulin-Binding B Domain, determined by NMR, 10 structures) was obtained from the RCSB Protein Data Bank (RCSB.org). The RCSB PDB is the U.S. data center for the global Protein Data Bank (PDB), which provides access to 3D structural data of large biological molecules such as proteins, DNA, and RNA-data that is essential for research and education in biology, health, energy, and biotechnology. The docking simulations were conducted using the Molecular Operating Environment (MOE) software (version 2015), a widely recognized tool for predicting molecular interactions and evaluating inhibition potential against target proteins [14]. The docking procedure was performed for all three compounds (HAP, CHI, GEN) in combination with the protein target. Before docking, the structures were prepared by adding hydrogen atoms using the Protonate3D function, repairing any missing bonds or connections, and minimizing the potential energy. The optimized 3D conformations of the ligands following the docking process are presented in Figure 2.

Additionally, the Site Finder tool was applied to identify the active sites on Protein A, and the processed protein structure along with the percentage of interacting residues is illustrated in Figure 3 [14]. The simulation produced 30 initial binding poses, which were evaluated using the London dG scoring function and subsequently refined twice using the Triangle Matcher placement method [14]. From these, the five poses with the best scores and interaction geometries were selected for further analysis. The significance of compound-compound and compound-protein interactions was assessed based on the hydrogen bond length (H-distance), which must be ≤ 3.5Å [14], and the energy score (S). Electrostatic potential maps were also generated to visualize the distribution of charge across the molecular surface and clarify the nature of the interactions within linear domains [15].

3. Results and discussion

3.1. Molecular properties

The optimized structures of Hydroxyapatite, Gentamicin, and Chitosan are represented in Figure 1.

3.2. Orbital study

We performed electronic structure calculations using Density Functional Theory (DFT) to analyze hydroxyapatite (HAP), chitosan (CHI), and gentamicin (GEN) to investigate

Table 3: 3D structures, score energy, and bond length H of HAP-CHI interaction.

Pose	S (energy score)	Distance (Å)	3D structures
1	-4.31	6.64	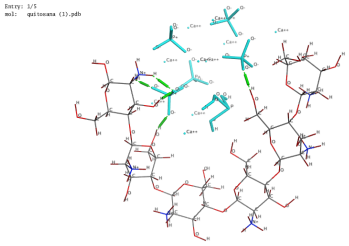
2	-4.26	5.01	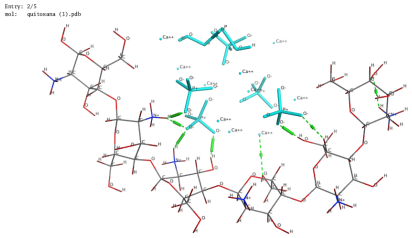
3	-3.90	4.37	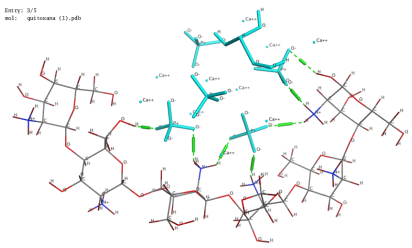
4	-3.88	3.43	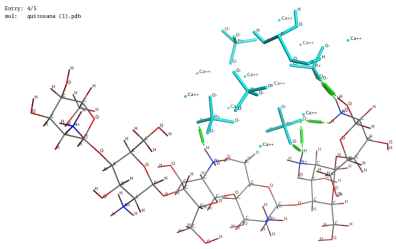
5	-3.86	4.24	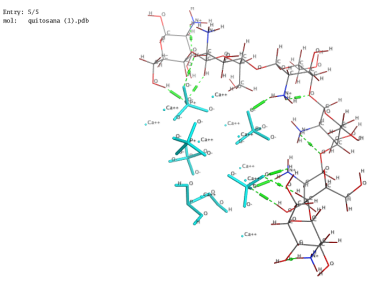

their chemical bonding characteristics in greater detail [20]. The energy gap between the highest occupied molecular orbital (HOMO) and the lowest unoccupied molecular orbital (LUMO), as defined in equation (1), is a critical parameter for assessing molecular stability. In addition to indicating chemical hardness (η, equation (2)) and softness (S, equation (3)), the HOMO-LUMO gap also reflects a molecule's electronegativity and chemical reactivity. Molecules with a small HOMO-LUMO gap are generally classified as soft; they are highly polarizable, chemically reactive, and exhibit low kinetic stability [21, 22]. The frontier molecular orbitals, HOMO and LUMO, play a key role in governing how a molecule interacts with other species [22]. The HOMO represents a molecule's tendency to donate electrons, while the LUMO indicates its capacity to accept electrons [9]. The HOMO and LUMO energies, energy gap (ΔE), absolute hardness (η), and softness (S) for HAP,

Table 4: 3D structures, score energy, and bond length H of HAP-GEN interaction.

Pose	S (Energy score)	Distance (Å)	3D structures
1	-3.18	10.48	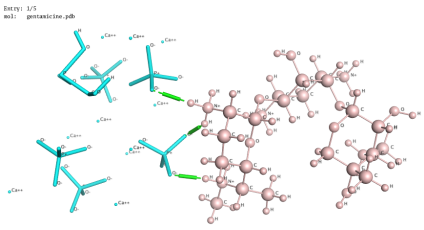
2	-3.01	4.51	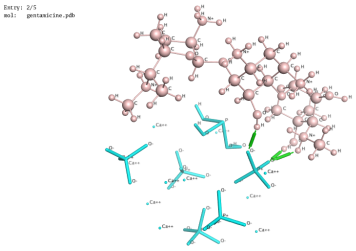
3	-2.94	8.78	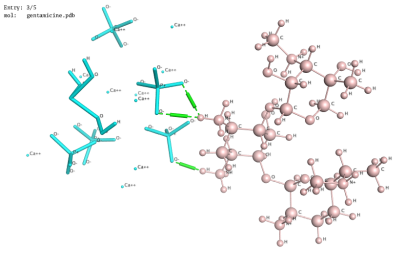
4	-2.80	6.35	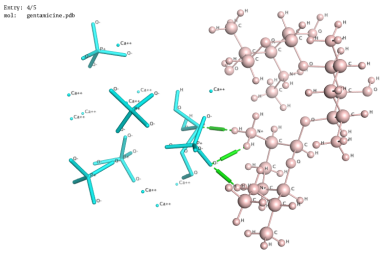
5	-2.78	9.30	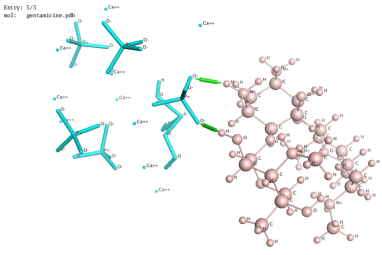

CHI, and GEN were computed using the DFT/B3LYP method, and the results are presented in Tables 1 and 2. Moreover, the molecular electrostatic potential (MEP) maps were generated to identify regions prone to nucleophilic and electrophilic attacks, following the approach described by Gamil A.A. Al-Hazmi et al. [15]. In the MEP visualizations of hydroxyapatite, chitosan, and gentamicin shown in Figure 4, three distinct colors are observed:

(i) Blue indicates electron-deficient (positively charged) regions, which are favorable for nucleophilic attack.

(ii) Red highlights electron-rich (negatively charged) areas, which are susceptible to electrophilic attack.

(iii) Green represents regions of neutral electrostatic potential.

Table 5: 3D structures, Score Energy, and bond length H of CHI-GEN interaction.

Pose	*S* (Energy score)	Distance (Å)	3D structures
1	-3.95	2.47	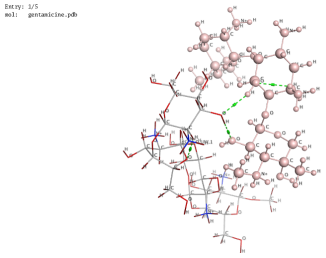
2	-3.53	4.36	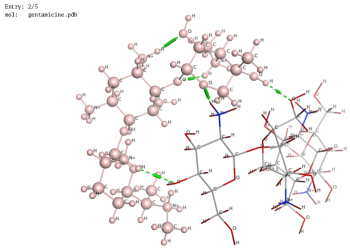
3	-3.48	5.33	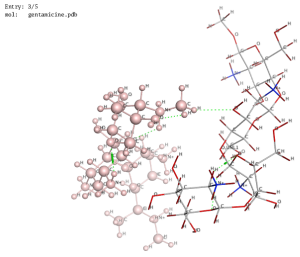
4	-3.33	3.72	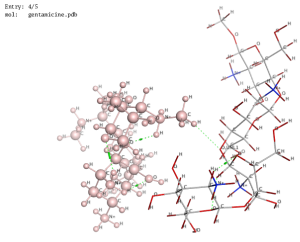
5	3.26	3.93	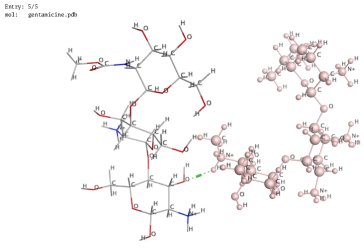

These visualizations help to better understand the reactivity and interaction potential of the compounds at the molecular level.

According to Tables 1 and 2, the three compounds-HAP, CHI, and GEN-exhibit a low HOMO-LUMO energy gap. As reported in the literature [21, 22], a low gap energy is associated with high polarizability, low kinetic stability, and high chemical reactivity. Therefore, HAP, CHI, and GEN can be classified as soft molecules [22]. As a result, electron transfer between the molecular orbitals of these compounds can occur more easily [23]. The Molecular Electrostatic Potential (MEP) maps in Figure 4 further support this analysis. They show that the oxygen atoms in chitosan (c) and gentamicin (b) represent the primary active (negatively charged) sites, which are favorable for interaction with hydroxyapatite (a), whose surface regions appear positively charged. This electrostatic complementarity facilitates the formation of stable interactions between the three

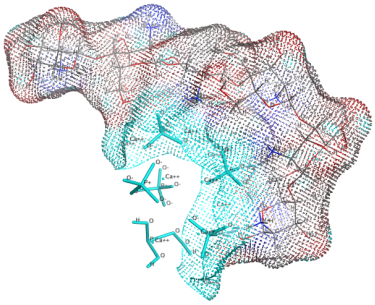

(a) Hydroxyapatite

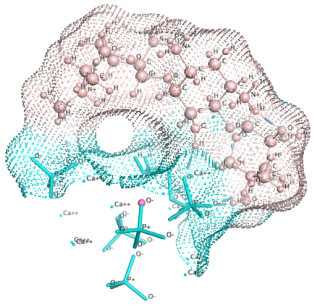

(b) Gentamicin

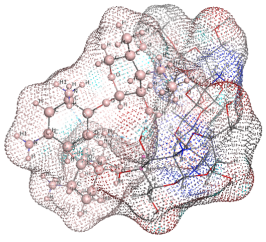

(c) Chitosan

Figure 5: Best interection of hydroxyapatite with chitosane (a), hydroxyapatite with gentamicin (b); and gentamicin with chitosane (c).

components.

3.3. Molecular operating environment (MOE)

The MOE Docking approach is one of the most widely adopted methods in the pharmaceutical industry for drug discovery, as it provides a virtual simulation of the interaction between a candidate compound (proposed drug) and a target pathogenic protein within the cell [24]. In this study, we employed this method for two main objectives: to investigate the molecular interactions between hydroxyapatite (HAP), chitosan (CHI), and gentamicin (GEN), and to theoretically evaluate the inhibitory effect of chitosan on Staphylococcus aureus Protein A, as well as to confirm, from a computational perspective, the antibiotic activity of gentamicin against the same protein, which plays a key role in osteomyelitis pathogenesis [4]. The interaction parameters are shown in Tables 3, 4, 5, 6, and 7.

- CHI with Protein A interaction (Table 6).
- GEN with protein A interaction (Table 7)

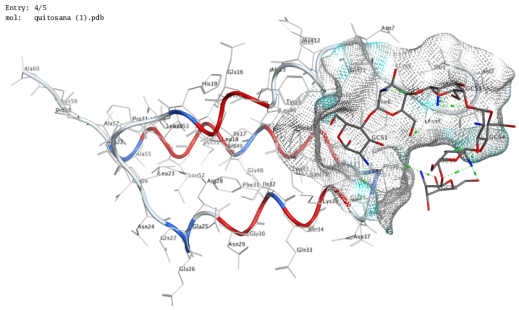

(a) Chitosan

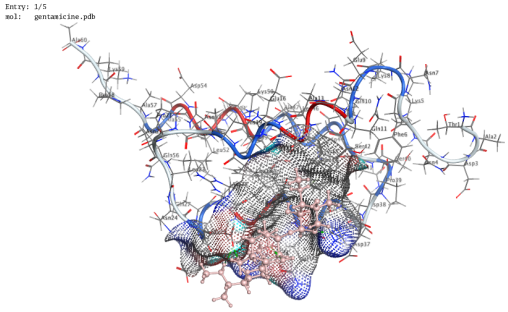

(b) Gentamicin

Figure 6: Surface maps of best interactions of Chitosan and gentamicin against protein A.

3.3.1. Interaction compound-compound

Molecular docking commonly predicts the binding orientation of drugs and small molecules. In this study, [25] we used MOE docking to compare the interaction of hydroxyapatite and chitosan as a drug delivery system for gentamicin. Three interactions are carried out: HAP-CHI, HAP-GEN, and CHI-GEN. The interaction parameters compared and discussed in this study are; ligand site, amino acid receptors, interaction type, bond length H (Distance (Å)), and scoring energy (S))) shown in Tables 3, 4, and 5, respectively. In addition, anchoring patterns, as well as electrostatic maps Figure 5 were deliberately examined to determine the degree and type of occlusion with amino acid receptors [15]. According to Tables 3, 4, and 5, the CHI-GEN interaction is the most important, with a lower H distance, especially in pose1 (2.47Å), and an average energy score (-3.95). These results mean that the binding of gentamicin to chitosan is stronger due to the hydrogen bonds formed, and the site of interaction of HAP and GEN is in the oxygen part. The electrostatic maps shown in Figure 5 confirm the importance of gentamicin's interaction with chitosan, reflected by the observable occlusion of chitosan's electron cloud with gentamicin's electron cloud [15].

3.3.2. Interaction compound-protein

CHI plays a significant role in the drug delivery system. According to the results obtained by Gaussian 09 of the interaction of CHI with HAP and GEN, CHI ensures the binding of GEN to HAP. This binding aims to build a complex to avoid osteomyelitis. We used Docking MOE to estimate the degree of inhibition of CHI and GEN against protein A, the el-

Table 6: 3D structures, score energy, and bond length H of CHI-Protein A interaction.

Pose	*S*	Rmsd-refine	3D structures
1	-7.18	2.31	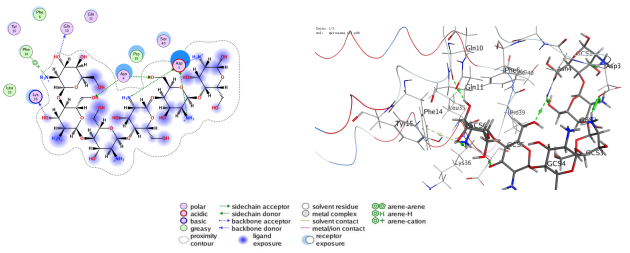
2	-6.92	2.55	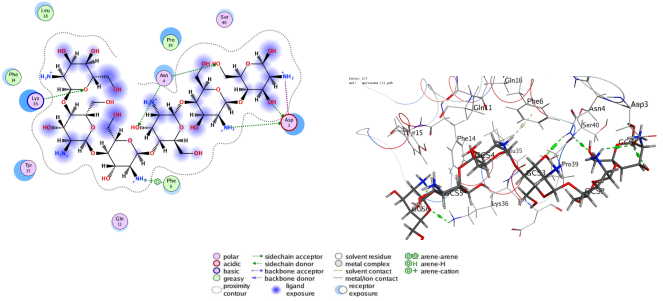
3	-6.89	6.91	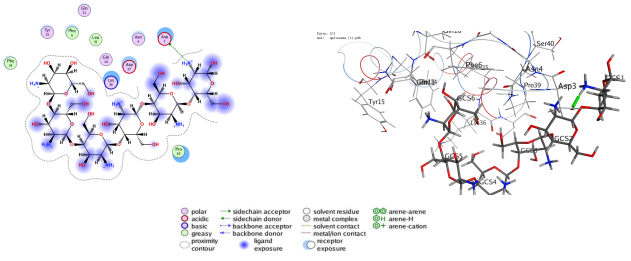
4	-6.87	1.49	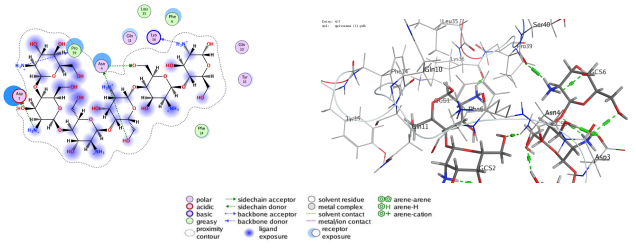
5	-6.85	5.11	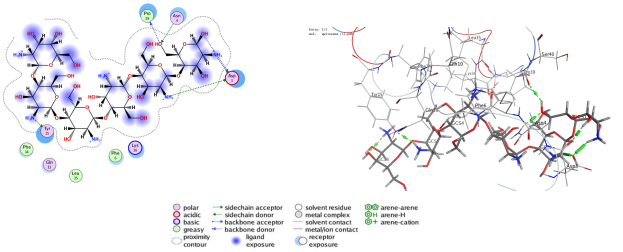

ement responsible for osteomyelitis. The tables below 6, and 7 present the interaction parameters of CHI and GEN compounds with Protein A, interaction validation schemes, and 3D structures. CHI shows moderate inhibition, with an average energy score of -6.94 and an average distance of 3.67 in the 5 poses extracted. The most important pose is pose 4, with a score of

Table 7: 3D structures, Score Energy, and bond length H of GEN- Protein A interaction

Pose	*S*	Rmsd-refine	3D structures
1	-5.28	2.07	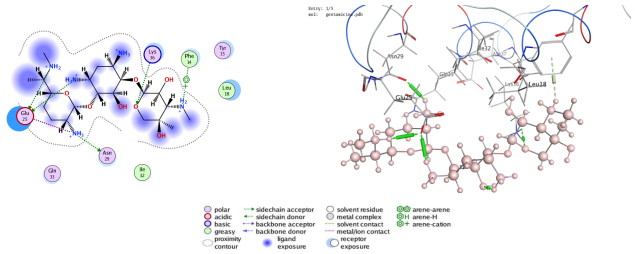
2	-5.25	1.13	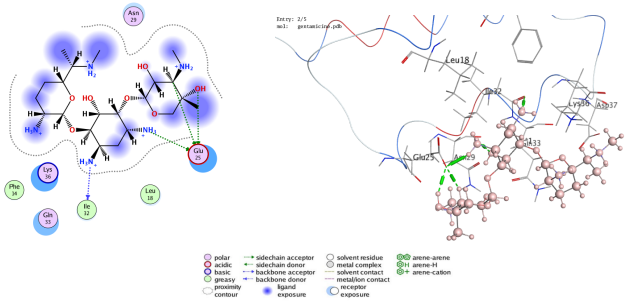
3	-5.25	1.55	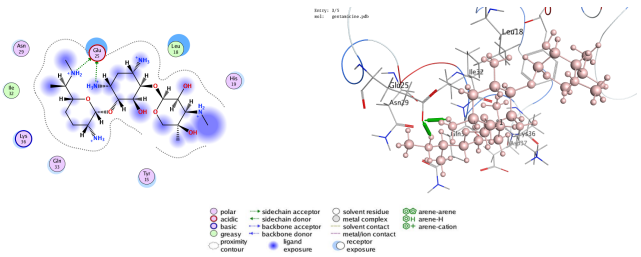
4	-5.16	2.61	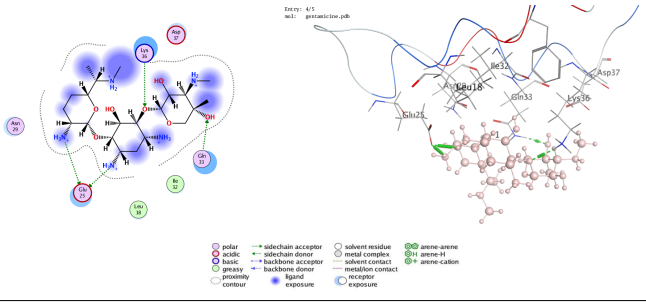
5	-5.14	1.29	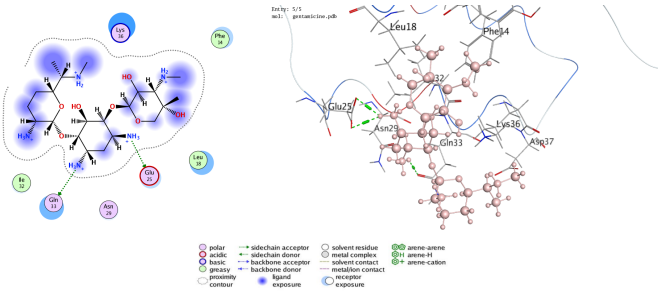

−6.87 and a distance of 1.49 ≤ 3.5Å, which according to the interaction validity schema makes 5 hydrogen interactions with amino acid residues: ASN4, which accounts for 13% of the protein A sequence, LYS35 (%10), ASP (%6.66) and Pro35 (%5).

Asparagine (ASN4) was found to establish two polar hydrogen bonds with two CHI oxygens. Lysine (LYS35) established a basic bond with the CHI nitrogen atom. Proline (Pro35) forms a greasy bond with the nitrogen atom.

GEN shows significant inhibition compared to CHI, with an average energy score of -5.21 and an average distance of 1.73 ≤ 3.5Å in the 5 extracted poses. These results are in accord with the experimental results of Stevanović *et al.* [7, 8]. The most significant pose is pose 1, with a score of -5.28 and a distance of 2.07Å, which, according to Schema interaction validity, establishes 6 hydrogen interactions with amino acid residues: ASN29, which accounts for 13% of the protein A sequence, LYS36 (%10), Glu25 (%8.3) and Phe14 (%5). Asparagine (ASN4) establishes a polar hydrogen bond with the CHI nitrogen atom. Lysine (LYS35) establishes a basic bond with CHI oxygen. Glutamine (Glu25) forms three acidic bonds with three nitrogen atoms.

Figure 6 shows the electrostatic maps of the best interactions of chitosan and gentamicin with protein A. An occlusion is observed for both ligands with the electron cloud in protein A [15].

4. Conclusion

In this study, based on DFT calculations and molecular docking simulations performed using Gaussian 09, the theoretical results show that electron movement between the orbitals of HAP, CHI, and GEN can easily occur due to the molecules' softness. Chitosan exhibits a higher binding affinity for gentamicin than hydroxyapatite, indicating a stronger CHI-GEN complex interaction. The primary interaction site between hydroxyapatite and gentamicin with chitosan is located on the oxygen atoms, identified as nucleophilic regions through electrostatic potential maps. Chitosan shows moderate inhibition against Protein A, with an average docking score of -6.94 and an average bond length of 3.67Å, close to the threshold (≤ 3.5Å) for significant interactions. In contrast, gentamicin shows stronger inhibition, with an average docking score of -5.21 and a shorter bond length of 1.73Å, confirming its high affinity for the target protein. These results suggest that chitosan plays a critical role in the drug delivery system by facilitating the binding of gentamicin to hydroxyapatite, due to the molecules' softness and the stronger interaction between CHI and GEN. This binding mechanism may be key to preventing Staphylococcus aureus-induced osteomyelitis. In conclusion, this theoretical study provides valuable insights into the interactions of biomaterials in drug delivery systems. It underscores the synergistic behavior of hydroxyapatite, chitosan, and gentamicin, and paves the way for innovative applications in biomedical fields, including the design of antibacterial implant coatings and targeted antibiotic delivery systems.

Data availability

The data will be available on request from the corresponding author.

References

[1] Y. Wang, J. Liu, C. Zhang, Y. Wang & T. Fan, "Recent development of chitosan-based biomaterials for the treatment of osteomyelitis", Journal of Polymer Engineering **44** (2024) 1437. https://doi.org/10.1515/polyeng-2023-0294.

[2] X. Ji, L. Gao, J. C. Liu, J. Wang, Q. Cheng, J. P. Li, S. Q. Li, K. Q. Zhi, R. C. Zeng & Z. L. Wang, "Corrosion resistance and antibacterial properties of hydroxyapatite coating induced by gentamicin-loaded polymeric multilayers on magnesium alloys", Colloids and Surfaces B: Biointerfaces **179** (2019) 429. https://doi.org/10.1016/j.colsurfb.2019.04.029.

[3] C. C. Yang, C. C. Lin, J. W. Liao & S. K. Yen, "Vancomycin-chitosan composite deposited on post porous hydroxyapatite coated Ti6Al4V implant for drug controlled release", Materials Sciences and Engineering C **33** (2013) 2203. https://doi.org/10.1016/j.msec.2013.01.038.

[4] L. L. Lima, P. R. Oliveira, V. C. Carvalho, S. Cimmerman & E. Savio, "Recommendations for the treatment of osteomyelitis", The Brazilian Journal of Infectious Diseases **5** (2014) 526. http://dx.doi.org/10.1016/j.bjid.2013.12.005.

[5] L. Zhang, K. Jacobson, J. Vasi, M. Lindberg & L. Frykberg, "Second IgG-binding protein in staphylococcus aureus", Microbiology **144** (1998) 985. https://doi.org/10.1099/00221287-144-4-985.

[6] J. J. Langone, "Applications of immobilized protein A in immunochemical techniques", Journal of Immunological Methods **3** (1982) 277. https://doi.org/10.1016/0022-1759(82)90088-6.

[7] M. Stevanovi, M. Dosic, A. Jankovic, M. Vukasinovic-Sekulic, J. Stojanovic, J. Odovic, M. C. Sakac, K. Y. Rhee & V. Miskovic-Stankovic, "Gentamicin-loaded bioactive hydroxyapatite/chitosan composite coating electrodeposited on titanium", ACS Biomaterials Science and Engineering **12** (2018) 3994. https://doi.org/10.1021/acsbiomaterials.8b00859.

[8] M. Stevanović, M. Djosić, A. Janković, V. Kojić, M. Vukasinovic Sekulić, J. Stojanović, J. Odovipac, M. C. Sakac, R. K. Yop & V. Miskovic Stanković, "Antibacterial graphene-based hydroxyapatite/chitosan coating with gentamicin for potential applications in bone tissue engineering", Journal of Biomedical Materials Research Part A **108** (2020) 2175. https://doi.org/10.1002/jbm.a.36974.

[9] I. Kara, Y. Kara, A. O. Kiraz & R. Mammadov, "Theoretical calculations of a compound formed by Fe+3 and tris(catechol)", Spectrochimica Acta - Part A: Molecular and Biomolecular Spectroscopy **149** (2015) 592. https://doi.org/10.1016/j.saa.2015.04.058.

[10] F. Gharibzadeh, E. Vessally, L. Edjlali, M. Es Haghi & R. Mohammadi, "A DFT study on sumanene, corannulene, and nanosheet as the anodes in li-ion batteries", Iranian Journal of Chemistry and Chemical Engineering **104** (2020) 51. https://doi.org/10.30492/ijcce.2020.106867.3568.

[11] D. T. Reis, S. Q. de Aguiar Filho, C. G. L. Grotto, M. F. R. Bihain & D. H. Pereira, "Carboxymethyl cellulose and cellulose xanthate matrices as potential adsorbent material for potentially toxic Cr3+, Cu2+, and Cd2+ metal ions: a theoretical study", Theoretical Chemistry Accounts **139** (2020) 96. https://doi.org/10.1007/s00214-020-02610-2.

[12] A. B. Cruz, N. N. Ciribelli, C. L. Cunha, I. R. Nascimento, J. C. Holzbach & D. H. Pereira, "Theoretical and experimental study of the diastereoisomers (2S) and (2R)-naringenin-6-C-?-D-glucopyranoside obtained from Clitoria guianensis", Journal of Molecular Modeling **29** (2023) 77. https://doi.org/10.1007/s00894-023-05482-y.

[13] S. Duran & S. T. Moin, "Chitosan nanoparticles as drug carrier of gentamicin-density functional theory and molecular dynamics simulation studies", Journal of Molecular Liquids **413** (2024) 125866. https://doi.org/10.1016/j.molliq.2024.125866.

[14] H. M. Abumelha, J. H. Al Fahemi, I. Althagaf, A. A. Bayazeed, Z. A. Al Ahmed, A. M. Khedr & N. El Metwaly, "Deliberate-characterization for Ni(II)-Schiff base complexes: promising in-vitro anticancer feature that matched MOE docking-approach", Journal of Inorganic and Organometallic Polymers and Materials **9** (2020) 3277. https://doi.org/10.1007/s10904-020-01503-y.

[15] G. A. A. Al-Hazmi, K. S. Abou-Melha, N. M. El-Metwaly, I. Althagafi, F. Shaaban & R. Zaky, "Green synthesis approach for Fe (III), Cu (II), Zn (II) and Ni (II)-Schiff base complexes, spectral, conformational, MOE docking, and biological studies", Applied Organometallic Chemistry **34** (2019) e5403. https://doi.org/10.1002/aoc.5403.

[16] M. Frisch, "Gaussian 09, revision d. 01, Gaussian", Inc., Wallingford CT **201**, 2009. [Online]. https://cir.nii.ac.jp/crid/1370298757422456580.

[17] T. A. Keith & M. J. Frisch, "Subshell fitting of relativistic atomic core electron densities for use in QTAIM analyses of ECP-based wave functions", Journal of Physical Chemistry A **115** (2011) 12879. https://doi.org/10.1021/jp2040086.

[18] D. T. Reis, I. H. S. Ribeiro & D. H. Pereira, "DFT study of the application of polymers cellulose and cellulose acetate for adsorption of metal ions (Cd2+, Cu2+ and Cr3+) potentially toxic", Polymer Bulletin **77** (2020) 3443. https://doi.org/10.1007/s00289-019-02926-5.

[19] H. Atmani, A. Aboulouard, F. E. Bakkardouch, L. Laallam, A. Jouaiti & M. El Edrissi, "Physical and chemical aspects of the interaction of chitosan and cellulose acetate with ions Ca2+ and K+ using DFT methods", Journal of Molecular Modeling **27** (2021) 103. https://doi.org/10.1007/s00894-021-04715-2.

[20] Z. Guerfi, O. K. Kribaa & H. Djouama, "Chemical-physical behavior of hydroxyapatite: a modeling approach", Journal of the Mechanical Behavior of Biomedical Materials **150** (2024) 106. https://doi.org/10.1016/j.jmbbm.2023.106229.

[21] K. Fukui, "Role of frontier orbitals in chemical reactions", Science **218** (1982) 747. https://doi.org/10.1126/science.218.4574.747.

[22] H. P. Gümü, Ö. Tamer, Avci D & Y. Atalay, "Quantum chemical calculations on the geometrical, conformational, spectroscopic and nonlinear optical parameters of 5-(2-chloroethyl)-2,4-dichloro-6-methyl pyrimidine", Spectrochimica Acta - Part A: Molecular and Biomolecular Spectroscopy **129** (2014) 219. https://doi.org/10.1016/j.saa.2014.03.031.

[23] R. Kurtaran, S. Odabaiolu, A. Azizoglu, H. Kara & O. Atakol, "Experimental and computational study on [2,6-bis(3,5-dimethyl-N-pyrazolyl)pyridine]-(dithiocyanato)mercury(II)", Polyhedron **17** (2007) 5069. https://doi.org/10.1016/j.poly.2007.07.021.

[24] S. C. Dey, M. Al-Amin, T. U. Rashid, M. Z. Sultan, M. Ashaduzzaman, M. Sarker & S. M. Shamsuddin, "Preparation, characterization and performance evaluation of chitosan as an adsorbent for remazol red", International Journal of Latest Research in Engineering and Technology **2** (2016) 52. https://d1wqtxts1xzle7.cloudfront.net/43711400/Chitosan$_RemazolRed-libre.pdf.

[25] N. Rahman, I. Muhammad, Gul-E-Nayab, H. Khan, M. Aschner, R. Filosa & M. Daglia, "Molecular docking of isolated alkaloids for possible glucosidase inhibition", Biomolecules **9** (2019) 544. https://doi.org/10.3390/biom9100544.